

# MAD the ESO multi-conjugate adaptive optics demonstrator

Enrico Marchetti<sup>a</sup>, Norbert Hubin<sup>a</sup>, Enrico Fedrigo<sup>a</sup>, Joar Brynnel<sup>a</sup>,  
Bernard Delabre<sup>a</sup>, Rob Donaldson<sup>a</sup>, Francis Franza<sup>a</sup>, Rodolphe Conan<sup>a</sup>, Miska Le Louarn<sup>a</sup>, Cyril  
Cavadore<sup>a</sup>, Andrea Balestra<sup>a</sup>, Dietrich Baade<sup>a</sup>, Jean-Louis Lizon<sup>a</sup>, Roberto Gilmozzi<sup>a</sup>, Guy Monnet<sup>a</sup>,  
Roberto Ragazzoni<sup>b</sup>, Carmelo Arcidiacono<sup>c</sup>, Andrea Baruffolo<sup>d</sup>, Emiliano Diolaiti<sup>c</sup>, Jacopo  
Farinato<sup>b</sup>, Elise Viard<sup>b</sup>, David Butler<sup>f</sup>, Stefan Hippler<sup>f</sup>, Antonio Amorim<sup>g</sup>

<sup>a</sup>European Southern Observatory - Karl-Schwarzschild-Str 2,  
D-85748 Garching bei München, Germany;

<sup>b</sup>Osservatorio Astrofisico di Arcetri - Largo E.Fermi 5, I-50125 Firenze, Italy;

<sup>c</sup>Dipartimento di Astronomia e Scienza dello Spazio, Universita' di Firenze, - Largo E.Fermi 5,  
I-50125 Firenze, Italy;

<sup>d</sup>Osservatorio Astronomico di Padova - Vicolo dell'Osservatorio 5, I-35122 Padova, Italy;

<sup>e</sup>Dipartimento di Astronomia, Univ. di Padova - Vicolo dell'Osservatorio 2, I-35122 Padova Italy;

<sup>f</sup>Max-Planck-Institute für Astronomie – Knigstuhl 17, D-69117 Heidelberg, Germany;

<sup>g</sup>Faculdade de Ciências de Universidade de Lisboa, Edifício C5, Campo Grande,  
1749-016 Lisboa, Portugal

## ABSTRACT

Multi-Conjugate Adaptive Optics (MCAO) is working on the principle to perform wide field of view atmospheric turbulence correction using many Guide Stars located in and/or surrounding the observed target. The vertical distribution of the atmospheric turbulence is reconstructed by observing several guide stars and the correction is applied by some deformable mirrors optically conjugated at different altitudes above the telescope.

The European Southern Observatory together with external research institutions is going to build a Multi-Conjugate Adaptive Optics Demonstrator (MAD) to perform wide field of view adaptive optics correction. The aim of MAD is to demonstrate on the sky the feasibility of the MCAO technique and to evaluate all the critical aspects in building such kind of instrument in the framework of both the 2<sup>nd</sup> generation VLT instrumentation and the 100-m telescope OWL.

In this paper we present the conceptual design of the MAD module that will be installed at one of the VLT unit telescope in Paranal to perform on-sky observations. MAD is based on a two deformable mirrors correction system and on two multi-reference wavefront sensors capable to observe simultaneously some pre-selected configurations of Natural Guide Stars. MAD is expected to correct up to 2 arcmin field of view in K band.

**Keywords:** Multi-Conjugate Adaptive Optics systems, wavefront sensors, layer oriented MCAO.

## 1. INTRODUCTION

Multi-Conjugate Adaptive Optics (MCAO, Beckers 1988 and 1989; Ellerbroek 1994) is working on the principle to perform wide field of view atmospheric turbulence correction using many Guide Stars (GS) surrounding the observed target. The light coming from the GSs is analyzed through wavefront sensors whose signals are used to reconstruct the atmospheric turbulence at the different heights which some deformable mirrors are conjugated to.

Different approaches for MCAO correction have been proposed in the latest years such as the atmospheric tomography (also called Global Reconstruction) both in the zonal (Tallon and Foy, 1990) and in the modal way (Ragazzoni, Marchetti and Rigaut 1999) and the Layer Oriented (Ragazzoni 2000; Ragazzoni, Farinato and Marchetti 2000). The modal tomography has been also experimentally verified on the sky (Ragazzoni, Marchetti and Valente 2000). These two approaches, in their basic concept, need different wavefront sensors (WFSs) in order to better optimize the appropriate atmospheric reconstruction.

---

\* [emarchet@eso.org](mailto:emarchet@eso.org), phone +49.89.32006458; fax +49.89.32006320; <http://www.eso.org>

The European Southern Observatory in collaboration with external research institutions is building an instrument prototype, the MCAO demonstrator (MAD, Hubin et al. 2002), to proof on the sky the feasibility of the MCAO technique using both the reconstruction approaches in the view of the future 2<sup>nd</sup> generation of the VLT instrumentation and the 100-meters telescope OWL (Gilmozzi et al. 1998; Dierickx and Gilmozzi 2000).

MAD, intended as a fast track project, will be installed at the Nasmyth focus of a VLT unit telescope and the actual timeline foresees to have the on-sky operations for early 2004 using only natural guide stars (NGSs). In this paper we present the conceptual design of MAD, introducing the top-level requirements and the technical specs, passing through the opto-mechanical concept, the WFSs, the corrective optics and the real-time computer. The contributions of three external collaborations are described: the Layer Oriented Wavefront Sensor, the high resolution large FoV infrared camera and the atmospheric turbulence generator. Finally the estimated correction performance for both the Global Reconstruction and Layer Oriented approaches will be given.

## 2. TOP LEVEL REQUIREMENTS AND TECHNICAL SPECIFICATIONS

MAD is a prototype MCAO system performing wide FoV AO correction over 2 arcmin on the sky by using bright ( $m_v < 14$ ) Natural Guide Stars (NGS).

MAD is implemented using existing technology and re-using as much as possible key components developed in the scope of existing AO systems.

MAD is used to investigate two different approaches of MCAO correction with two independent wavefront sensing techniques: the Star Oriented MCAO with a Shack-Hartmann WFS (SHWFS) sensing simultaneously 3 NGS with 3 SH WFS and the Layer Oriented MCAO with a Layer Oriented Wavefront Sensor (LOWFS) based on a Multi-Pyramid WFS (Ragazzoni 1996), sensing simultaneously 8 NGS. The MAD Real-Time computer architecture is designed in order to support both reconstruction approaches.

The MAD correction is based on two deformable mirrors (DM). One mirror is conjugated at the telescope pupil for ground layer turbulence correction, the second is conjugated at 8.5 Km above the telescope aperture enabling a larger FoV correction. The MAD MCAO correction is optimized for the K (2.2.  $\mu\text{m}$ ) band for the median seeing conditions and the performance will be evaluated at this wavelength.

MAD uses a 1 arcmin FoV IR camera, called CAMCAO, to evaluate the correction performance in K Band. During the laboratory testing it is foreseen to use the ESO IR Test Camera (ITC) with smaller FoV (17 arcsec).

For the testing and tuning of the MAD system, it is planned to install MAPS (Multi Atmospheric Phase screens and Stars), the multi-layer turbulence generator, at the input focus of MAD.

MAD will be installed at the Nasmyth focus of a VLT telescope unit.

## 3. OPTICAL LAYOUT

The optical design concept of MAD is provided below in Figure 1. The MAD input beam is F/15. A Field of View (FoV) of 2 arcmin is de-rotated by an optical derotator and collimated by a doublet lens (C-1) to re-image a telescope pupil of 60 mm in diameter. A 100 mm DM is conjugated at an altitude of 8.5 Km (DM-2) and a 60 mm DM is conjugated to the re-imaged telescope pupil (DM-1). A Tip-Tilt Mount (TTM) is supporting the DM-1 for the tip-tilt correction. A dichroic transmits the Infrared (IR) light (1 – 2.5  $\mu\text{m}$ ) toward the IR cameras and reflects the visible light (0.45 - 0.95  $\mu\text{m}$ ) toward the Wavefront Sensor (WFS) path. A lens objective provides a flat, telecentric F/20 input beam to the wavefront sensor.

Two WFSs are planned to be used with MAD: a Multi Shack-Hartmann (SHWFS) and a Layer Oriented WFS (LOWFS part of these specifications). Two different IR cameras are planned to be successively installed on the MAD bench:

- The CAMCAO (Camera for Multi-Conjugate Adaptive Optics demonstrator) which consists of a  $2\text{k} \times 2\text{k}$  IR detector fed by a cooled reflective optical train. The CAMCAO input beam is F/15 and the FoV is 1 arcmin.
- An Infrared Test Camera (ITC) which consists of a  $1\text{k} \times 1\text{k}$  IR detector fed by cooled reflective optical train. The ITC input beam is F/15 and the FoV is 17 arcsec.

To provide the corresponding F/ratio to both the IR cameras, a second collimator copy of C-1 is placed in the collimated beam after the dichroic. A scanning unit to patrol the 2 arcmin FoV with both IR cameras shall be provided.

The turbulence generator MAPS is located in proximity of the input F/15 to inject the turbulence inside the optical train. Two AO calibration units are implemented: one at F/15 input focus (Calibration Unit 1) and one at the input of the WFS optical path (Calibration Unit 2). These units consist of a set of movable illuminated fibers.

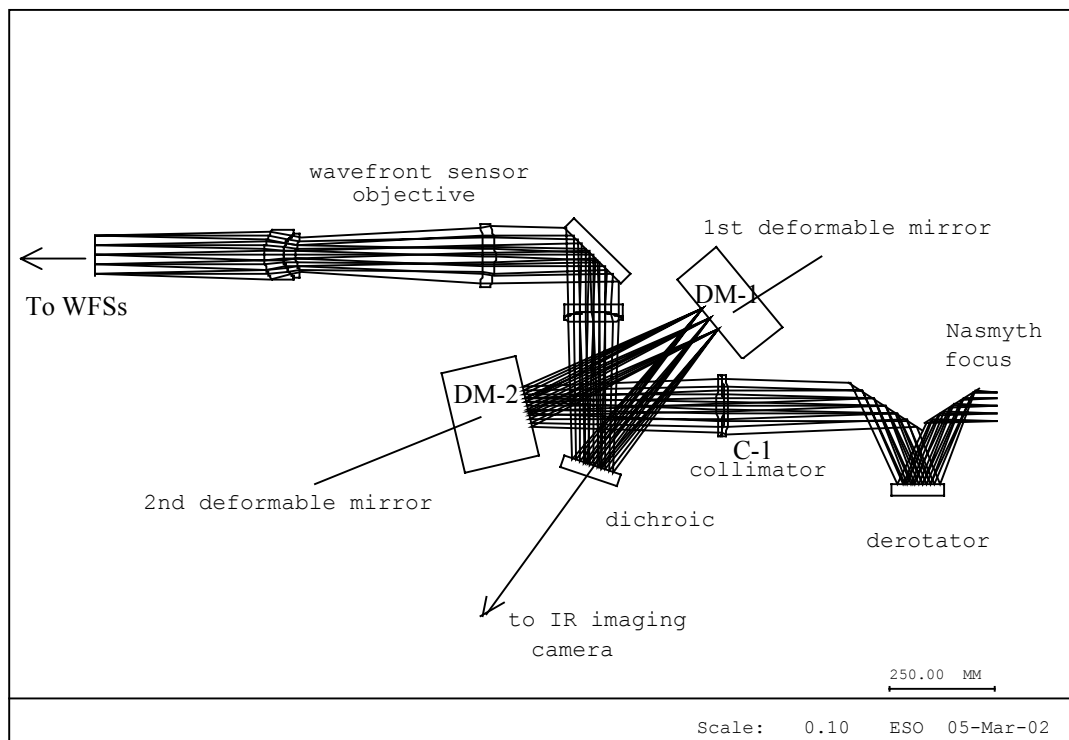


**Figure 1 Optical concept for the ESO MCAO Demonstrator**

#### 4. MECHANICAL LAYOUT

The Mechanics general assembly is shown in Figure 2. The opto-mechanical bench is placed on the Nasmyth platform and supported by legs. The optical derotator is a copy of the VLT spectrograph CRIRES one with optics adapted to transfer 2 arcmin FoV. The optics will be shaped to fit into the optical derotator, and will be made of aluminum. The WFS objective is supported by a dedicated structure including all the main optics. In the WFS area are located both WFSs. The WFSs are accommodated in order to have the focal plane parallel to bench plane. A WFS selector provides to fold the light to one OR the other WFS. The two WFS don't work at the same time. A third position of the WFS selector lets the light pass through toward the Acquisition camera. The Acquisition camera is used to image the whole 2 arcmin FoV in order to measure the positions of the NGSs for an accurate WFSs acquisition. The SHWFS is located on the bench and it is looking upward. The LOWFS box is mounted above the SHWFS and it is looking downward. Both the CAMCAO IR Camera and the ITC camera are located below the bench looking up through a hole in the table. A folding mirror and a collimator provide to bend and to focalize the light into the cameras. MAPS is supported by an optical table anchored to the MAD bench with proper support legs. The MAPS bench will be removed before the installation of MAD at the telescope.

Two calibration units are foreseen for MAD. The Calibration Unit 1 @ the F/15 input focus. This Calibration Unit consists of 8 visible-IR light illuminated fibers supported by a plate. The plate can be moved to scan the whole 2 arcmin FoV to emulate different NGS positions. A third motion along the optical axis will compensate for VLT field curvature. The calibration unit is moved out from the FoV during MAD close loop operations. The Calibration Unit 2 @ the WFS path has the same motions and fibers of the previous one and it is located below the table. A collimator provides to collimate the beam to be injected into the WFS objective after the deformable mirrors and before the dichroic. A sliding mirror can be inserted in the optical train to feed the WFS objective with this calibration unit. The fibers are illuminated by one or more lamps providing a broad band spectrum illumination from 0.5 to 2.5  $\mu\text{m}$ . The uniformity of the illumination of the fibers is guaranteed by using an integrating sphere located below the table and feeding both calibration units.

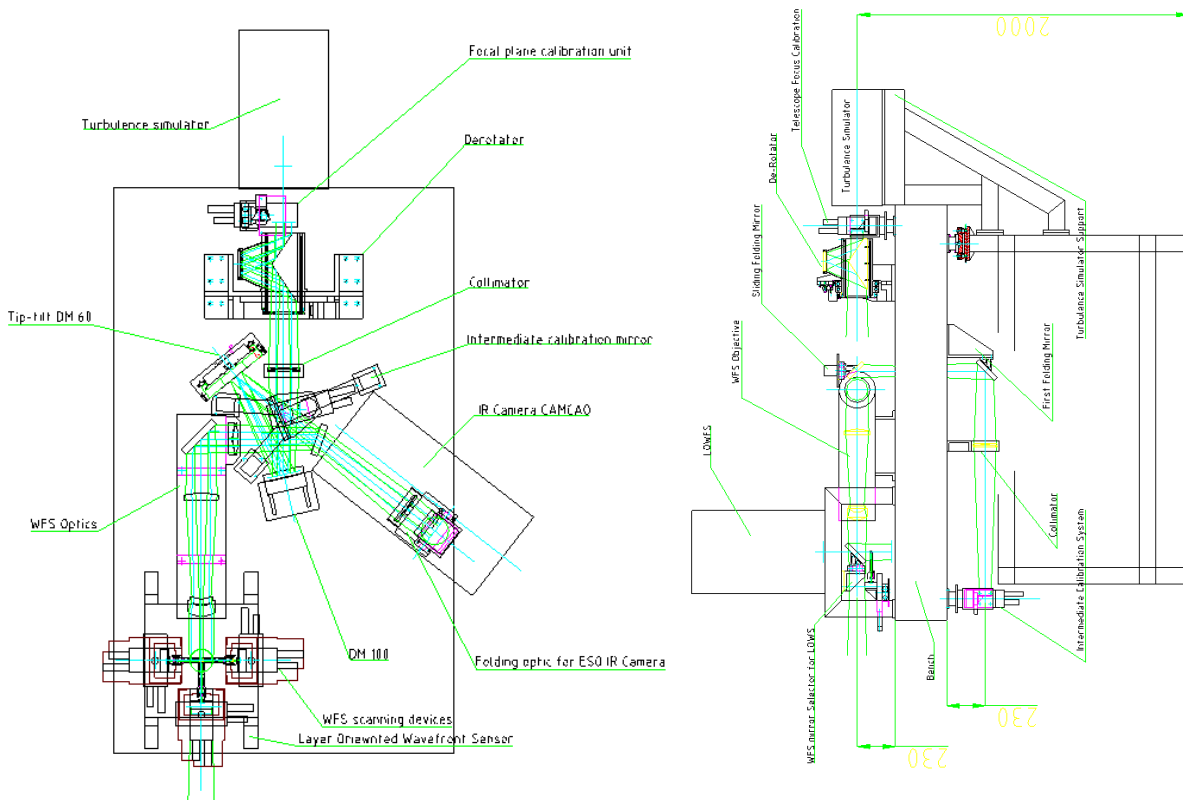


Figure 2 General Assembly – Top and side view

## 5. WAVEFRONT SENSORS

### 5.1. Multi Shack-Hartmann WFS

The Multi SHWFS consists of 3 Shack-Hartmann units (SHU) capable to scan the whole 2 arcmin FoV to pick-up the NGSs for the wavefront sensing (see Figure 3). Each SHU is provided with an arm supporting a pick up mirror folding the light through the SHU optics, a FoV diaphragm of 2.4 arcsec located at the F/20 focus and doublet lens that re-images the telescope pupil on the lenslet array. The lenslet array is an  $8 \times 8$  sub-apertures,  $192 \mu\text{m}$  pitch, 3.2 mm focal length. Each small lens focuses the NGS light on the WFS camera detector over  $8 \times 8$  pixels,  $24 \mu\text{m}$  size (scale 0.3 arcsec/pixel).

Each SHU is mounted on a XY motion scanning the 2 arcmin FoV and the three arms are slightly displaced in altitude with respect to the table plane in order to avoid mutual collisions.

### 5.2. Layer Oriented WFS

The LOWFS is based on a multi pyramid WFS with eight pyramids to observe simultaneously eight NGSs. The conceptual design is shown in Figure 4. Each pyramid is supported by a small cylinder containing some re-imaging optics to enlarge the system focal ratio by a factor  $\sim 10$  on the top of the pyramid. The light modulated by the pyramid is then re-imaged through two groups of lenses and the pupil image of the observed NGS is created on the plane where the WFS camera detectors are located. Between the two group of lenses a dichroic splits the light toward two WFS cameras slightly displaced along the optical axis in order to provide the footprint geometries proper of the conjugation altitudes of the two DMs of MAD.

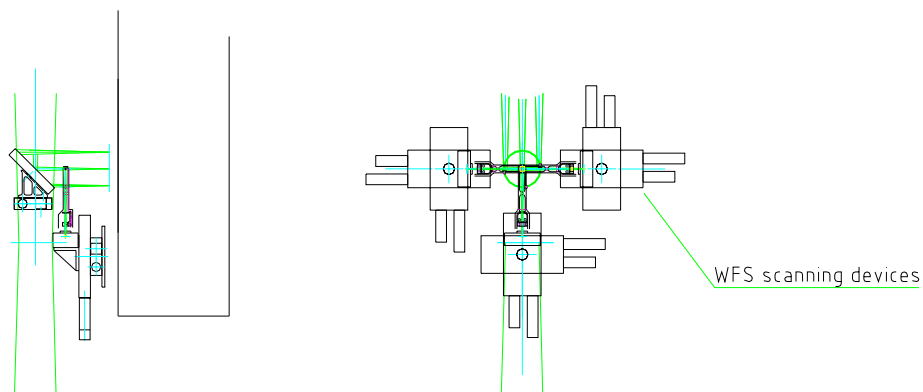


**Figure 3 Mechanical layout of the Multi SHWFS. Left: side view, SHU and WFS selector folding the light into the SHU. Right: top view, the three SHUs.**

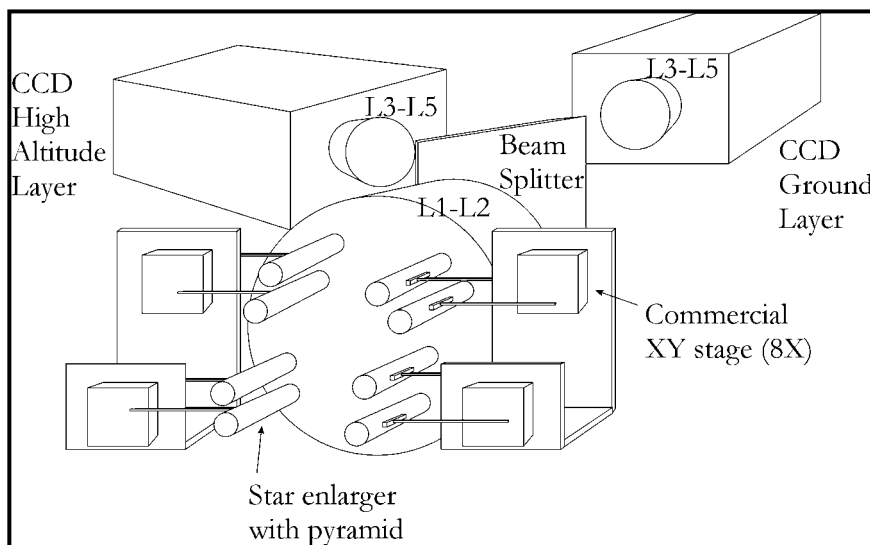


**Figure 4 Layer Oriented WFS conceptual design**

### 5.3. Detector System

The MAD detector system consists of 5 WFS cameras (3 for the SHWFS and 2 for the LOWFS) based on the Marconi CCD50 chip especially developed for the NAOS system. Only one CCD50 quadrant will be used, that is,  $64 \times 64$  pixel ( $24 \mu\text{m}$ ) and 4 outputs.

The CCD50 chips are mounted inside a small compact CCD heads, three of them including the lenslet array (SFWFS), and the detector is cooled down to  $-40^\circ\text{C}$  by a Peltier cooler.

The CCD50 are controlled by a FIERA system. For the SHWFS 12 outputs will be used simultaneously, for the LOWFS only 8 outputs. For the SHWFS, FIERA will be able to drive the detectors simultaneously at the same frame rate while for the LOWFS it is required to run the two detectors at different frame rates. The maximum frame rate required is 400 Hz. The read-out modes are taken from those developed for NAOS. FIERA will not drive the two WFS at the same time.

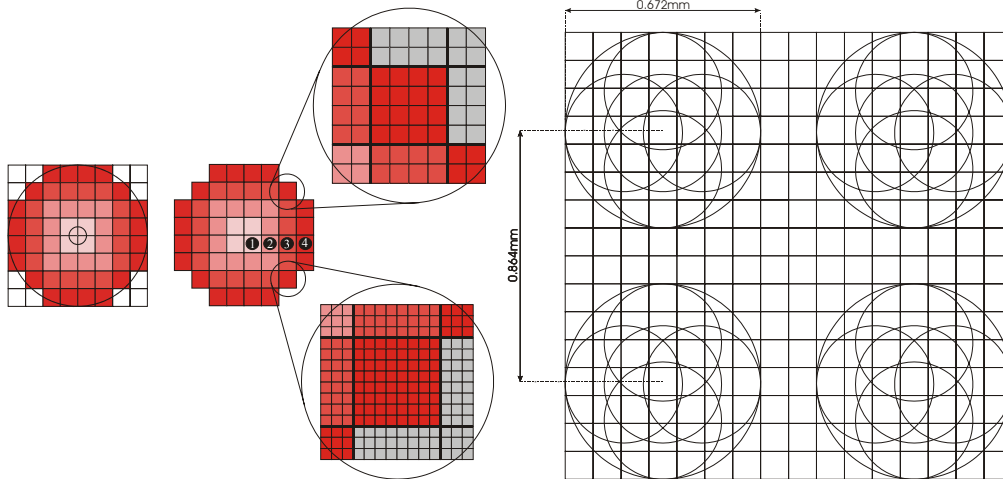


**Figure 5 Sub-aperture layout with respect to the CCD50 detectors for the SHWFS (left) and for the LOWFS (right)**

The layouts of the sub-apertures geometry for both the WFSs are shown in Figure 5. In the SHWFS the useful surface of the detectors is divided in  $8 \times 8$  sub-apertures,  $8 \times 8$  pixels each. The number of useful sub-apertures is 52. In the LOWFS the detector conjugated with the ground layer has a fixed binning of  $2 \times 2$  while the detector conjugated at 9.2 Km has a fixed binning of  $4 \times 4$ . Taking into account the difference of the footprint size of the 2 arcmin FoV at the two altitudes, for the ground conjugated detector the resulting sub-aperture grid is  $8 \times 8$ , while for the high altitude conjugated one is  $7 \times 7$ .

#### 5.4. Acquisition Camera

The Acquisition Camera is based on an ESO Technical CCD (TCCD,  $1024 \times 1024$ ,  $24 \mu\text{m}$ ) coupled to a lens objective for the acquisition of the whole 2 arcmin FoV. The resulting scale on the detector is  $\sim 0.10$  arcsec/pixel optimal for accurate NGS centroid measurements. The aim of the acquisition camera is to provide the WFSs with a precise measurement of the NGSs location for accurate positioning of both the SHU and the pyramids.

### 6. DEFORMABLE MIRRORS

The Deformable Mirror conjugated to the ground the MACAO SINFONI/CRIRES bimorph DM, 60mm pupil, radial geometry (see Figure 6). The Deformable Mirror conjugated to the altitude of 9.2 Km is the MACAO-VLTI bimorph DM, 100mm pupil, radial geometry (see Figure 6).

The tip-tilt correction is provided by the SINFONI/CRIRES Tip-Tilt supporting the MACAO SINFONI/CRIRES DM.

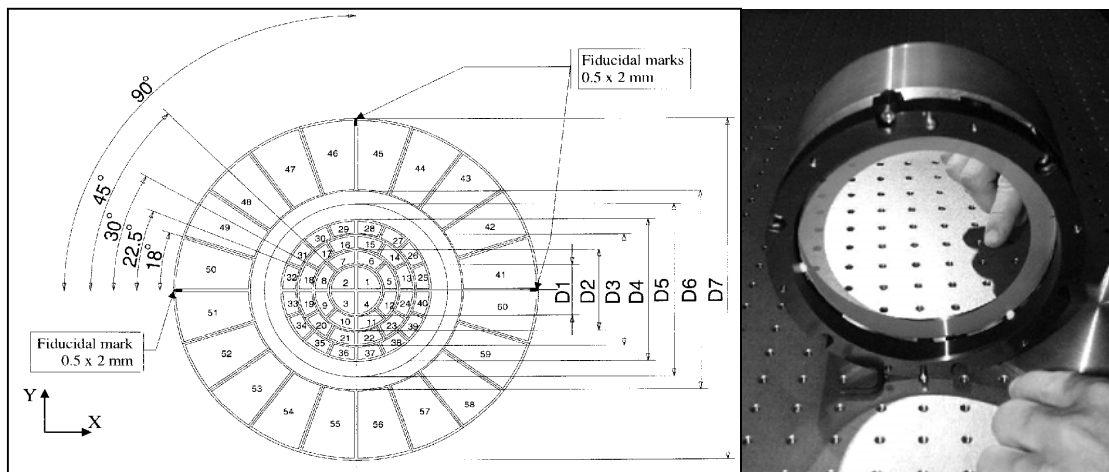


**Figure 6 Geometry of the sub-apertures in the MAD Deformable Mirrors (left) and MCAO-VLTI DM (right)**

## 7. REAL-TIME COMPUTER

The MAD Real-Time Computer Hardware architecture is shown in Figure 7. A standard ESO instrument workstation (WS) is used to interface to the Local Control Unit (LCU) and hosting the WS components of the MAD RTC SW. It will run other WS components of the MAD system.

The supervisory Computer (LCU) is a PowerPC (PPC) 604, the current version running at 400 MHz but replaceable in the future with faster releases, mountable in a VME rack. It has a RS232 serial link going to the High Voltage Amplifier for housekeeping operations.

The Real-Time Computer is the Dy4 CHAMP-AV board, a Quad-G4 board that mounts 4 PowerPC 7410 running at 500 MHz. The connection between the RTC and FIERA is assured by a 32 bit digital I/O board

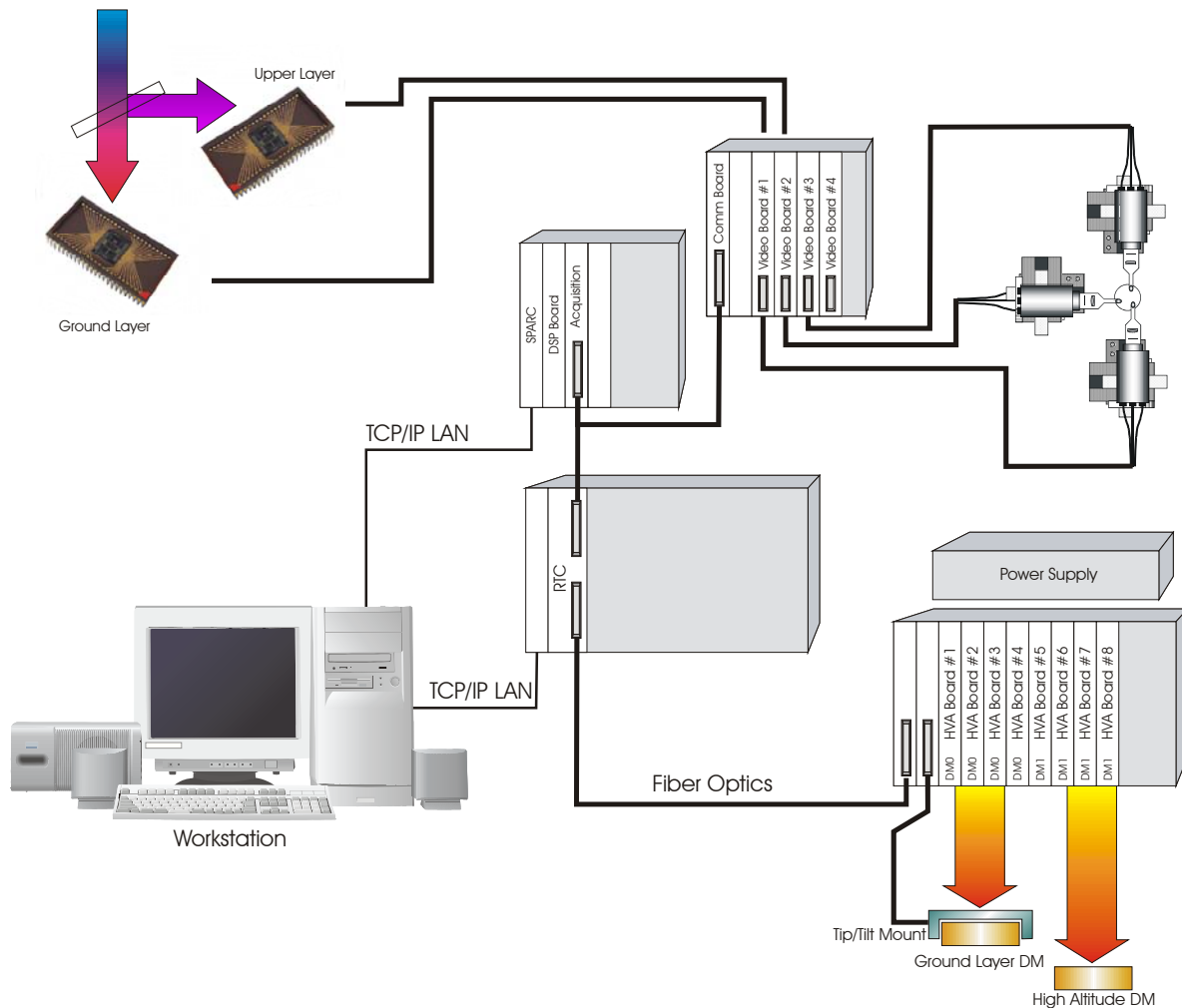


**Figure 7 Real-Time Computer architecture**

In the case of the SHWFS, the signals of the three SHUs are sent together to the RTC for the slope computation. The control commands are the extrapolated for three channels: DM1, DM2 and Tip-Tilt, filtered and sent to the corresponding correcting units. The three channels are parallelized. Each channel needs the signals from all the SHUs to be executed.

In the case of the LOWFS, the signals from the detector conjugated to one layer are sent to the RTC for the slope computations. The control commands are computed, filtered and sent to the corresponding correcting DM. The signals from the other detector follow the same process to command the other DM. The two processes are independent and are executed in parallel. Each process is related only to the corresponding detector. Part of the control commands is taken from both the channels to drive the Tip-Tilt mount.

## 8. CONTROL ELECTRONICS

The MAD Control Electronics overview is shown in Figure 8. The main instrument control LCUs are:

- The LCU to control the optical derotator, the bench motions, the SHWFS motions and the calibration unit lamps.
- The LCU is used to control the LOWFS motions
- The LCU is used to control the TCCD.
- The FIERA UltraSparc controls the WFS camera of both the WFSs.
- The LCU is used to control the RTC, the DMs High Voltage Amplifiers, and the TTM.
- The IRACE UltraSparc is used to control the CAMCAO and ITC IR cameras.

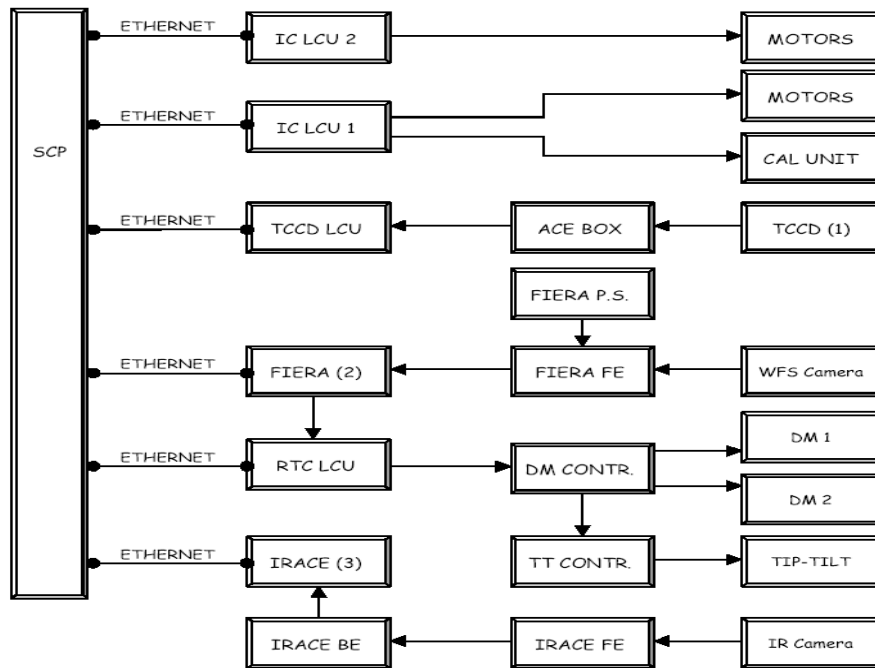


Figure 8 MAD Control Electronics Overview

## 9. OBSERVING AND INSTRUMENT CONTROL SOFTWARE

The MAD software architecture is shown in Figure 9. MAD includes a number of separate subsystems under software control, these subsystems are:

- **Science Camera** Two different science cameras will be use alternately, one imaging a ~1' FoV and one imaging a 17" FoV both are read out by an IRACE controller. The standard IRACE DCS SW and RTD are used with no additional development. The small field science camera will be mounted on two linear axes to allow it to scan the complete 2' field (TBC).
- **Wavefront Sensor (WFS) Detector** Either two CCDs for the Layer Oriented wavefront sensor or three CCDs for the Shack-Hartmann wavefront sensor read out by a FIERA CCD controller. Only one of the wavefront sensors at a time can be connected to FIERA, switching between them requiring manual rewiring. The standard FIERA DCS SW and RTD are used with new readout modes provided by the ODT.
- **Acquisition Camera** A standard large TCCD imaging the complete 2' FoV for visualising and refining reference star locations. The standard TCCD DCS SW and RTD are used without modification.
- **Real-Time Computer** The real-time computer acquires wavefront sensor data from the FIERA controller, applies the AO control algorithm, drives the corrective optics and provides display facilities for imaging the WFS data.



- **Instrument Control** Driving the motorised functions and calibration units, based on the VLT standard ICS “icb”.
- **Observing Software**

The software which coordinates the activities of the other MAD subsystems. Based on the VLT standard OS “BOSS”. The OS in turn is driven by MAD specific templates which are scheduled by the Broker of Observation Blocks (BOB).

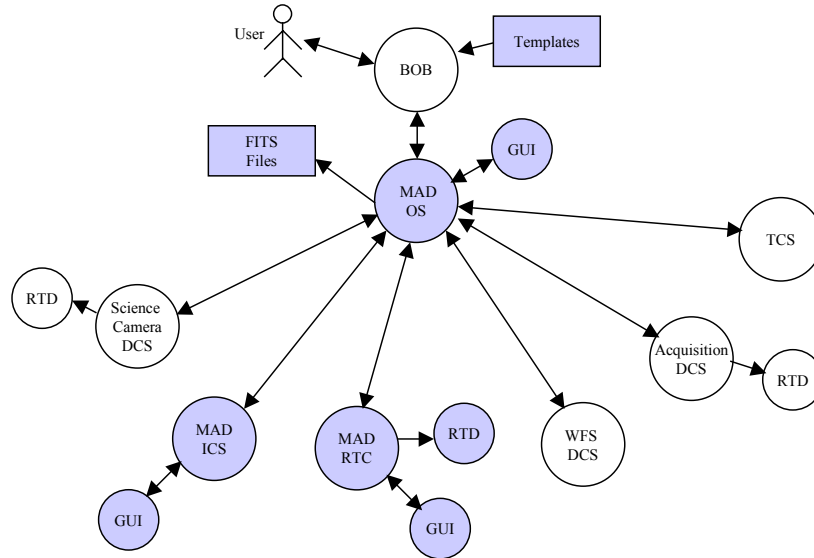


**Figure 9 MAD Software architecture**

## 10. CAMCAO INFRARED CAMERA

The CAMCAO IR camera is a 1 arcmin FoV camera with pixel scale of 0.028 arcsec/pixel (Nyquist sampling in K Band). CAMCAO is used to evaluate the wide FoV MCAO correction of MAD.

CAMCAO is based on a  $2k \times 2k$  Hawaii2 IR detector controlled by a standard IRACE system. The camera will have standard IR band filters mounted on a manually positionable filter wheel. CAMCAO is placed in F/15 beam after the dichroic and it is provided with a cooled optical system, based only on spherical mirrors, shown in Figure 10. Field and pupil cold stops are implemented to significantly reduce the infrared background and the stray-light. The CAMCAO optics provide diffraction limited performance down to J Band, but the detector sampling allows diffraction limited imaging in K band.

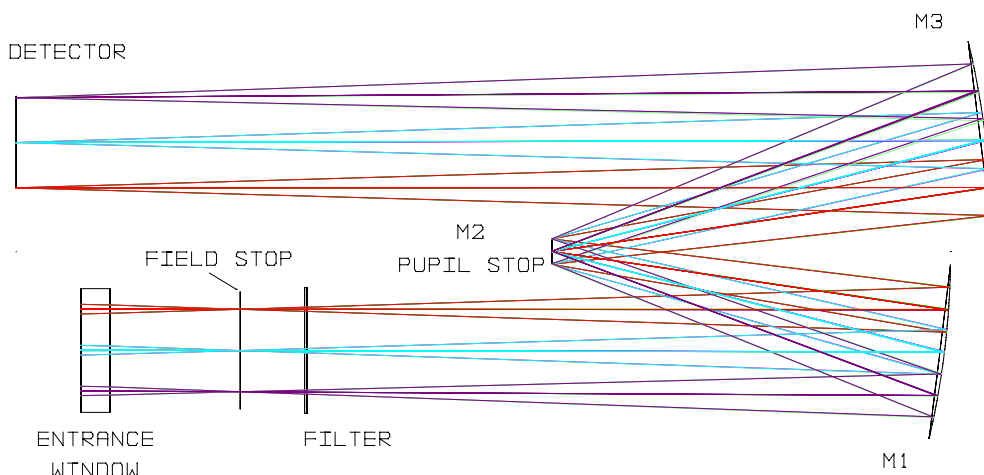


**Figure 10 CAMCAO optical design**

## 11. TURBULENCE GENERATOR MAPS

The MAPS goal is to emulate a time evolving three-dimensional atmosphere whose induced aberrations are injected into MAD. The characteristics of the atmospheric turbulence shall be similar to those of the Paranal observatory during median seeing conditions. The evolving atmosphere is reproduced by some rotating transmissive plates, called Phase Screens (PS). The refractive index in the PS substrate is modified locally in order to produce a phase shift in an electromagnetic wave passing through it.

A concept of MAPS is given in Figure 11. The Natural Guide Stars (NGS) are emulated by visible-IR light transmissive fibers. The fiber positions will be changeable to create the desired star configuration in a FoV of 2 arcmin. A first group of lenses collimates the light beams from the NGSs and allows the telescope pupil to be created. Different PSs are located in the collimated beams to emulate the atmospheric layers at different altitude. One phase screen is located close to the telescope pupil to emulate the ground layer. The PSs have different turbulence power according to the expected vertical distribution. The evolving atmosphere is emulated by rotating the PSs at different speeds according to the wind speed vertical profile. The PS separations and positions can be varied in order to modify the atmospheric anisoplanatism and the speeds can be adjusted to reproduce a wide range of atmospheric correlation times.

Moreover the PS are interchangeable in order to emulate a selected range of seeing conditions.

A second group of lenses re-images the artificial NGSs whose wavefront quality is degraded by the PSs. The distorted wavefronts are then injected into MAD for MCAO correction. MAPS is used only for laboratory testing

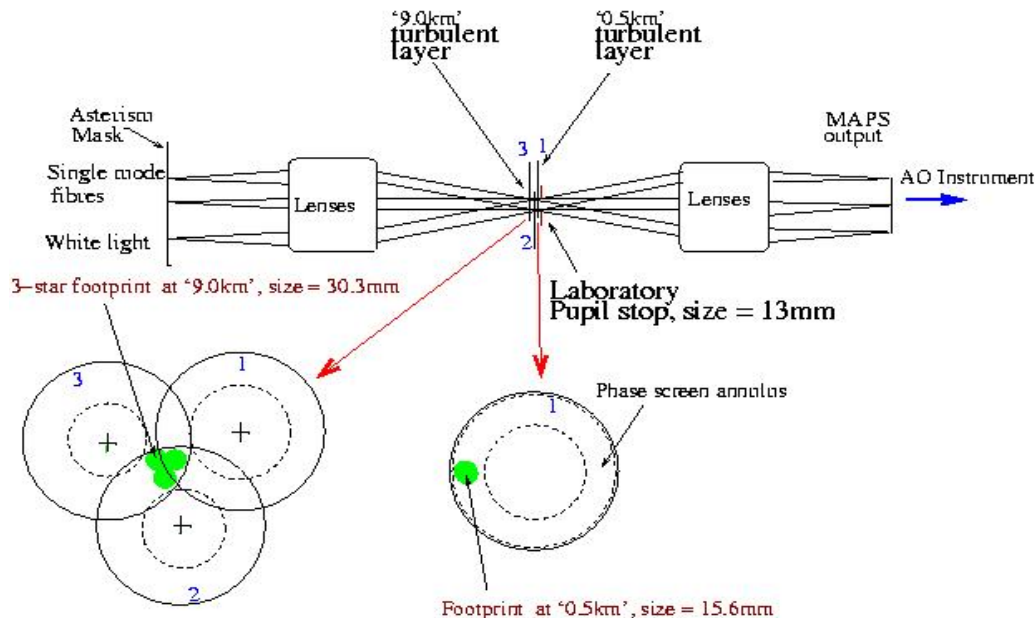


Figure 11 MAPS Conceptual Design

## 12. CORRECTION PERFORMANCE

Extensive numerical and analytical simulations have been implemented for simulating the MAD system in its Star Oriented mode with the Multi SHWFS and the LOWFS. The basic simulation parameters taken into account are:

- **Telescope pupil diameter:** 8 m
- **Atmosphere:** Seeing 0.67 arcsec @ 0.5  $\mu\text{m}$  at Zenith, Outer scale: 22 m. Seven layers Cerro Pachon model
- **Sky background:**  $m_v = 20 \text{ mag/arcsec}^2$
- **Wavefront sensors wavelength:** V band (0.55  $\mu\text{m}$ )
- **Deformable mirrors:** MACAO radial geometry, conjugation altitude 0 and 8.5 Km.
- **CCD detector:** RON < 6 e<sup>-</sup>/pixel, Dark: 500 e<sup>-</sup>/pixel/sec, QE: 82%, Bandwidth: 0.5  $\mu\text{m}$
- **Corrected Zernike modes:** 55

- **Correcting wavelength:** K band (2.2  $\mu\text{m}$ )
- **Zero Point:**  $1.0 \times 10^{11}$  photons/ $\text{m}^2/\text{sec}/\mu\text{m}$  for a star of  $m_v=0$
- **Total system throughput:** 0.20 including the detector QE and bandwidth

The correction performances are evaluated in K (2.2  $\mu\text{m}$ ) band and are given in Peak Strehl and maximum Strehl variation ( $\Delta$  Strehl) across the FoV at the Zenith and at a Zenithal distance of 30 degrees.

### 12.1. Multi SHWFS simulations

For the Multi SHWFS two types of simulations have been implemented. A full numerical simulation and an analytical simulation with an optimization algorithm to uniformed the correction of the whole FoV. The results are shown in Table 1 and Table 2 for two FoV amplitudes: the three NGSs are distributed on a circle of 1 and 2 arcmin of diameter.

Configuration	Star Oriented WFS	
	Peak Strehl / $\Delta$ Strehl@zenith	Peak Strehl / $\Delta$ Strehl@30°
3 NGSs, $M_v=12$ , equidistributed on a circle of diameter:		
1 arcmin	0.45 / 0.21	TBD
2 arcmin	0.31 / 0.21	0.28 / 0.13

**Table 1 Strehl Ratio obtained with numerical simulations**

Configuration	Star Oriented WFS + optimization @ 30°		
	SR optimized for one direction in the FoV	Peak Strehl / $\Delta$ Strehl optimized for 1' FoV	Peak Strehl / $\Delta$ Strehl optimized for 2' FoV
3 NGSs, $M_v=12$ , equidistributed on a circle of diameter:			
1 arcmin @ 30°	0.62	0.62/ 0.07	0.56/0.24
2 arcmin @ 30°	0.42	0.44/ 0.03	0.48/0.28

**Table 2 Strehl Ratio obtained with the analytical simulations and optimization algorithm for correction at 30° from Zenith**

### 12.2. LOWFS simulations

For the LOWFS several cases have been analyzed with variable number and brightness of NGS. In Figure 12 is shown an example of Strehl map obtained for the NGSs contained in an asterism centered in RA 10h 35m 50.1s and dec  $-58^\circ 12' 50''$ , of galactic latitude  $0^\circ$ . The stars are arranged in two arcmin field. The integrated magnitude of the asterism is 5 but different cases of integrated magnitude are considered dimming proportionally all the stars in order to obtain different integrated magnitudes. The results are summarized in Table 3.

Fov [°]	$M_v$ Int	$\Delta t$ integration on WF sensors	$\Delta t$ long exposure	Gains	SR on axis long exp.	Max SR long exp.	Max Instant. SR	$\sigma_{SR}$ over FoV	$\Delta$ SR over FoV
120	10	2.5 ms, 5 ms	1.5 sec	0.6, 0.6	0.33	0.44	0.57	0.06	0.37
120	11	10 ms, 5 ms	1.6 sec	0.6, 0.6	0.32	0.43	0.57	0.06	0.35
120	12	5 ms, 10 ms	1.5 sec	0.6, 0.6	0.30	0.41	0.57	0.06	0.35
120	13	10 ms, 10 ms	1.5 sec	0.6, 0.6	0.26	0.37	0.54	0.07	0.33
120	14	5 ms, 20 ms	1.5 sec	0.6, 0.6	0.19	0.28	0.43	0.06	0.26

**Table 3. Results of the simulations of the asterism with 8 stars of integrated magnitude  $M_v=10-14$**

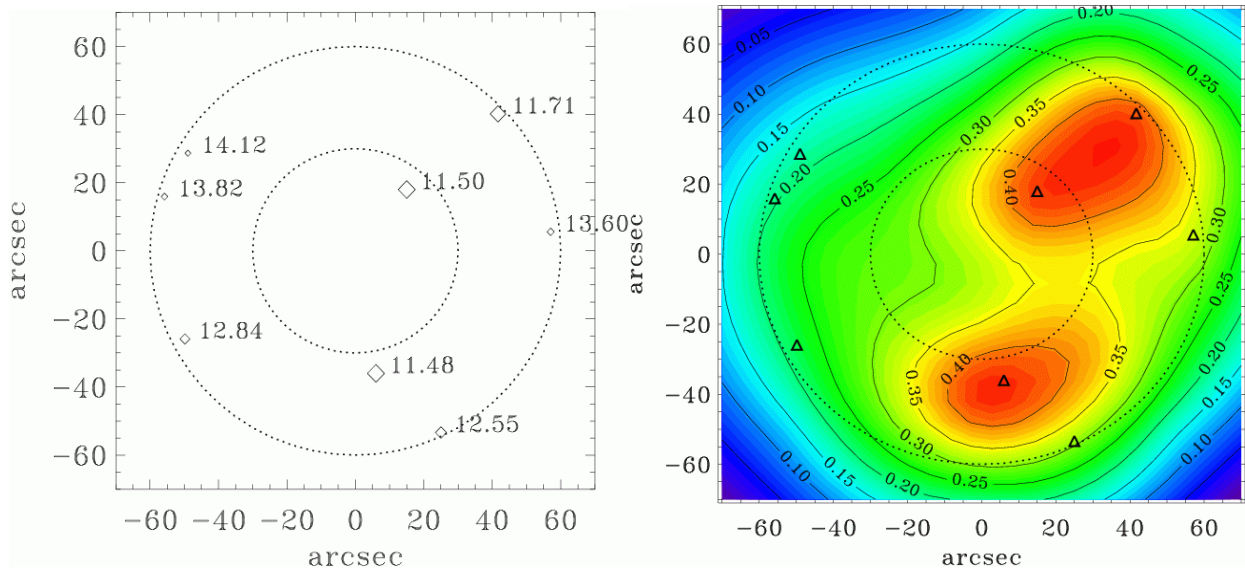


**Figure 12. Guide stars and SR map of the case with 8 stars asterism over two primes FoV, with integrated magnitude of the NGS  $M_V=10$ . In this case the optimal gain used was 0.6 for both DM, and the integration times used for WFSs were 2.5 ms for ground DM and 5.0 ms for high DM.**

### ACKNOWLEDGEMENTS

Thanks are due to R.Gilmozzi, G. Monnet and P.Dierickx for their strong support in the development of the project.

### REFERENCES

1. Beckers J. M., "Increasing the size of the isoplanatic patch size with multiconjugate adaptive optics", in *ESO conference on Very Large Telescopes and their instrumentation*, M.-H. Ulrich, ed., pp. 693, 1988.
2. Beckers J. M., "Detailed compensation of atmospheric seeing using multiconjugate adaptive optics", *Proc. SPIE* **1114**, pp. 215-217, 1989.
3. Dierickx P., Gilmozzi R., "OWL concept overview", in *ESO Proceedings of the Bäckaskog Workshop on Extremely large Telescopes* **57**, T.Andersen, A.Ardeberg and R.Gilmozzi, eds., pp. 43-52, 2000.
4. Ellerbroek B., "First order performance evaluation of adaptive optics system for atmospheric turbulence compensation in extended field-of-view astronomical telescope", *J. Opt. Soc. Am A* **11**, pp. 783-805, 1994.
5. Gilmozzi R., Delabre B., Dierickx P., Hubin N., Koch F., Monnet G., Quattri M., Rigaut F., Wilson R.N., "Future of filled aperture telescopes: is a 100-m feasible?", *Proc. SPIE* **3352**, pp. 778-791, 1998.
6. Hubin N., Marchetti E., Fedrigo E., Conan R., Ragazzoni R., Diolaiti E., Tordi M., Rousset G., Fusco T., Madec P.-Y., Butler D., Hippler S., Esposito E., "The ESO MCAO demonstrator MAD: a European collaboration", *ESO Proceedings of the Venice Conference on Beyond Conventional Adaptive Optics*, R.Ragazzoni, S.Esposito and N.Hubin, eds., in press, 2002.
7. Ragazzoni R., "Pupil plane wave front sensing with an oscillating prism", *J. of Mod. Opt.* **43**, pp. 289-293, 1996.
8. Ragazzoni R., Marchetti E. and Rigaut F., "Modal tomography for adaptive optics", *A&A* **342**, pp. L53-L56, 1999.
9. Ragazzoni R., "Adaptive optics for giants telescopes: NGS vs. LGS", in *ESO Proceedings of the Bäckaskog Workshop on Extremely large Telescopes* **57**, T. Andersen, A. Ardeberg and R. Gilmozzi, eds., pp. 175-180, 2000.
10. Ragazzoni R., Marchetti E. and Valente G., "Adaptive-optics correction available for the whole sky", *Nature* **403**, pp. 54-56, 2000.
11. Ragazzoni R., Farinato J. and Marchetti E., "Adaptive optics for 100-m-class telescopes: new challenges require new solutions", *Proc. SPIE* **4007**, pp. 1076-1087, 2000.
12. Tallon M. and Foy R., "Adaptive telescope with laser probe - Isoplanatism and cone effect", *A&A* **235**, pp. 549-557, 1990.